Analysis of High Speed P-I-N Photodiodes S-Parameters by a Novel Small-Signal Equivalent Circuit Model

G. Wang, T. Tokumitsu, *Member, IEEE,* I. Hanawa, K. Sato, and M. Kobayashi

***Abstract*—A novel small-signal radio frequency (RF) equivalent-circuit of the side-illuminated input tapered waveguide-integrated p–i–n photodiodes (WG PIN PD) is proposed. The proposed RF equivalent-circuit involves both the carrier-transit effect and the external resistance–capacitance (RC) time constant limitation on the frequency response of the p-i-n PD. The carrier-transit effect is realized by adding an RC circuit to an ideal voltage-controlled current source as the input opto-RF equivalent circuit. The carrier transit-time effect is equivalently represented by the time-constant of this input RC circuit. This new equivalent circuit model fits well with both the measured reflection and optoelectronic conversion parameters of the WG PIN PD in a broad frequency range from 45 MHz to 50 GHz.**

***Index Terms*—Equivalent circuits, photodiodes, scattering parameters.**

I. Introduction

RECENTLY, next-generation optical-fiber communication systems operated at 40 Gb/s per channel have been intensively developed [1], which has created a new demand for high-speed photodiodes (PDs). To satisfy the requirement for both high sensitivity and high-speed response, a side-illuminated input tapered waveguide-integrated p-i-n N PD (WG PIN PD) with a 3-dB bandwidth of over 40 GHz has been developed [2]. In the meantime, there was a need for evaluating the opto-microwave properties of high-speed PDs. S parameters are widely used microwave parameters for characterizing and modeling high-frequency and high-speed devices with readily available measurement equipment. It is very important for high-speed PD designer, at minimum, to obtain small-signal equivalent-circuit element values from the measured S parameters. However, any effective and measurement-based opto-microwave equivalent circuits have not been reported, to our best knowledge.

In this letter, we proposed a novel small-signal radio frequency (RF) equivalent circuit for the WG PIN PD, which is considered on both the carrier-transit effect and the external resistance–capacitance (RC) time constant. This proposed PIN PD equivalent circuit produced a good approximation with the measured reflection coefficients (S_{22}) and the optoelectronic conversion properties (S_{21}) of the devices in a broad frequency range from 45 MHz to 50 GHz.

Manuscript received March 7, 2002; revised May 9, 2002. The review of this letter was arranged by Associate Editor Dr. Shigeo Kawasaki.

The authors are with Fujitsu Quantum Devices Limited, Kokubo Kogyo Danchi, Yamanashi-ken, Japan.

Digital Object Identifier 10.1109/LMWC.2002.804557.

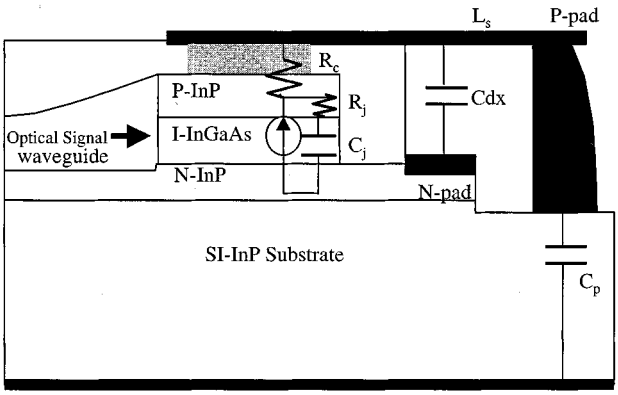

Fig. 1. Cross section of a side-illuminated input tapered waveguide-integrated PIN PD. The equivalent circuit elements are related to the PIN PD parameters as shown.

II. Equivalent Circuit Design

Fig. 1 shows the cross-sectional view of the side-illuminated p^+-InP/I–InGaAs/n-InP double-hetero junction WG PIN PD that uses input tapered waveguide and air-bridge technology. The p-i-n junction area is 6×7 μm^2 and the thickness of InGaAs absorption layer is 0.28 μm. The details are described in reference [2]. Fig. 1 also indicates how the equivalent-circuit components are connected and related to the physics parameters of the WG PIN PD, where R_c is the p-electrode contact resistance; R_j is the resistance of P^+-InP layer; C_j is the reverse bias junction capacitance; Cdx is the capacitance between the air-bridge and n-electrode pad; C_p is the p-electrode pad capacitance; and L_s is the inductance of the air-bridge from p-contact to p-electrode pad. Rearranging the equivalent circuit components shown in Fig. 1 gives an RF small-signal equivalent circuit shown in Fig. 2(a), that is, a half portion of the WG PIN PD model, where L_g is the inductance induced by the n-electrode pad as RF ground pattern. As only an extremely small dark current is flowed under a reverse bias of -5 V, the shunt resistance across the current source is ignored in this equivalent circuit.

The optical-to-microwave conversion frequency response in a photodiode is limited by both the carrier-transit time and the external parasitic RC time constant. The small-signal RF equivalent circuit shown in Fig. 2(a) can be used to evaluate the effect of the external parasitic RC time constant. As for the effect of carrier-transit time, it is usually necessary to study the physical aspects of the devices by a complicated numerical simulation [3]. Now, we analyze the transit time effect in the deple-

tion (drift) region. We may consider the illuminated light as an equivalent cathode emitting free carriers, which induces a photo current. Since the illuminated light contains both dc and ac components, the induced photo current includes both dc current I_D and ac current I_{RF}. The total ac current I_{RF} flowing through the drift region of the p-i-n diode consists of two components: the displacement current and the spatial dependent conduction current. Following an analysis given by Wang [4] for a reverse biased PIN IMPATT avalanche diode, I_{RF} is given by

$$I_{RF} = i\omega\varepsilon E(\omega) + \gamma I_{RF}\exp(-i\omega x/v_s). \tag{1}$$

The first part in (1) is the displacement current, where the $E(\omega)$ is the ac component of the field in the drift region, γ is the ratio of the ac conduction-current to the total ac current, and v_s is the constant saturation drift velocity of the carrier in the drift region, respectively. For PIN PD, v_s represents the saturation drift velocity of the carrier generated in the depletion region even for low level illumination, while it is dependent on optical input power level. By solving the $E(\omega)$ in (1) and integrating it over the drift region, we can obtain the ac voltage V_{RF} across the drift region and equivalently represent the drift region by an impedance Z_d as

$$Z_d = R + iX = \frac{V_{RF}}{I_{RF}}. \tag{2}$$

When the WG PIN PD is used for high-power and high-speed operation, there will be nonuniformity in charge distribution and as such nonuniformity on electric field and transition velocity, hence justification has to be made using IMPATT (1) for the p-i-n photodiode. However, the basic concept of using a linear circuit with an impedance Z_d is effective to equivalently represent the carrier-transit time for relatively small signal operation. This approximation well explained the high frequency response of the WG PIN PD based on (2) and an assumption that a couple of PD bandwidth-limiting factors induced by carrier-transit time and RC-time constant are independent of each other [5]. A small-signal RF equivalent circuit considering both the carrier-transit effect and the parasitic RC time constant for WG PIN PD is newly modeled, as shown in Fig. 2(b). In the model, an RC [indicated as R_tC_t in Fig. 2(b)] equivalent circuit with an impedance of Z_d is combined to the input side of the equivalent circuit Fig. 2(a) through a voltage-controlled current source. In the same figure, R_0 is the representation of the source impedance and the value was set at 50 Ω. The WG PIN PDs 3-dB bandwidth limited by the carrier transit-time effect can be approximated as the time constant determined by the input R_tC_t equivalent circuit. The ac photocurrent flow out to the external parasitic circuit was controlled by the ac voltage V_{RF} across this R_tC_t equivalent circuit. Hence, the current source is represented as g_mV_{RF}, where g_m is a constant adjusted to the opto-microwave conversion quantum efficiency. The validity of the above approximation will be proved in the next section.

III. Measurement and Analysis

Here, we determine the current output port as ② and the optical signal input port as ①, as shown in Fig. 2.

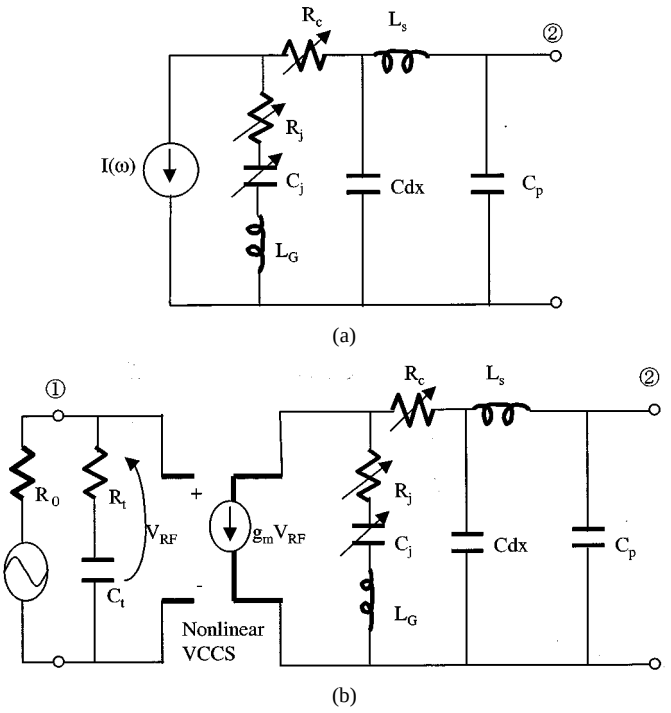

Fig. 2. Small-signal radio frequency model of the side-illuminated input tapered waveguide-integrated PIN PD: (a) equivalent circuit that only involves the parasitic elements and (b) equivalent circuit that involves both the parasitic elements and carrier transit-time effect.

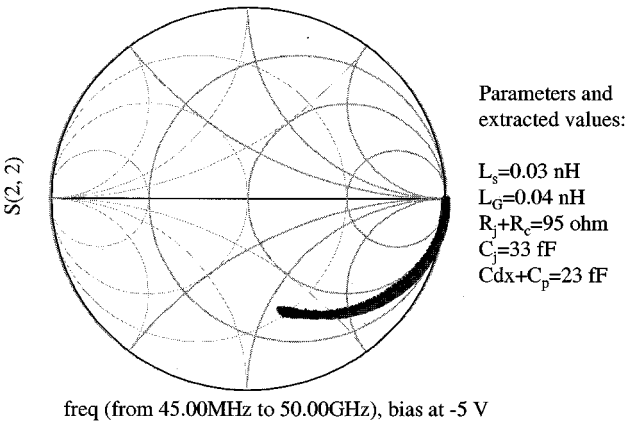

Fig. 3. Measured and calculated S_{22} (normalized to 50Ω) versus frequency (from 45 MHz to 50 GHz) of the side-illuminated input tapered waveguide-integrated PIN PD on Smith chart.

Fig. 3 shows the measured and calculated S_{22} versus frequency (from 45 MHz to 50 GHz) of the WG PIN PD structure on Smith chart. The small-signal equivalent circuit elements shown in Fig. 2(a) was extracted by best fitting the calculated S_{22} parameter to the measured S_{22} parameter across the measured frequency range. The best-fitting exhibited an exact adjust between the measured and calculated values, where the maximum fitting error levels in magnitude and phase difference of S_{22} are below 0.02% and $\pm 5^\circ$, respectively. The extracted values are also shown in Fig. 3. The total series resistances of less than 100 Ω and the total shunt capacitance of less than 60 fF at -5 V closely agree with those for dc measurement.

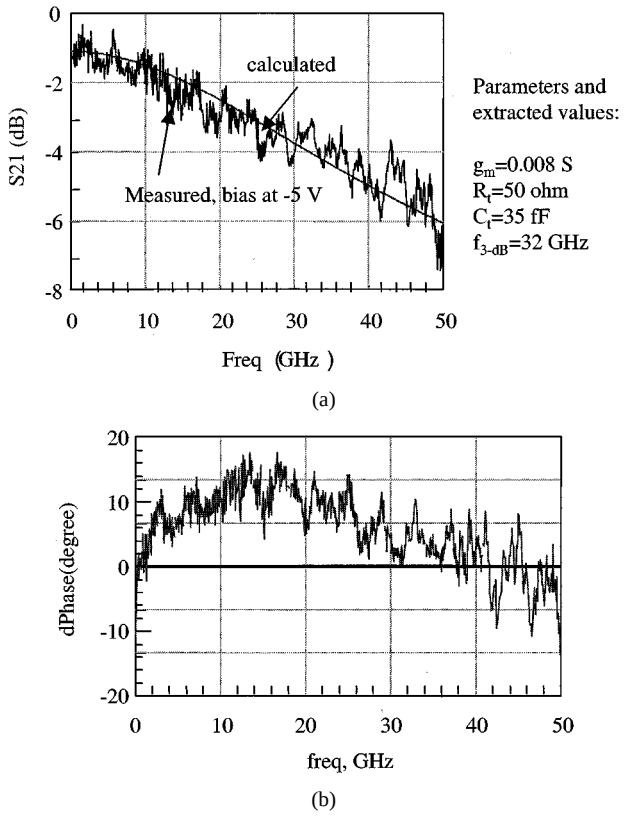

Fig. 4. (a) Measured and calculated optical-microwave conversion parameters S_{21} of the side-illuminated input tapered waveguide-integrated PIN PD. (b) The phase difference $(dPhase)$ of S_{21} between the measured and calculated values.

Frequency-domain optical responses were measured by a 50-GHz lightwave component analyzer equipment. The laser with a 1550-nm center wavelength was used as the measurement source. The device was contacted by GSG microwave probe with a 50-Ω load. Fig. 4 shows the measured frequency response (S_{21}) of the WG PIN PD. The optical input power was 1 mW (0 dBm). In order to evaluate the influence of the carrier transit-time effect, the values of the input circuit element [C_t, R_t and g_m in Fig. 2(b)] were chosen so that the calculated S_{21} curve can be best fitted with the measured S_{21} curve. The calculated S_{21} curves are shown in Fig. 4(a) with solid curve. The calculated 3-dB bandwidth $f_{3\text{-dB}}$ of 32 GHz for this sample well agrees to the measured one. The maximum fitting error levels in magnitude and phase difference between measured and calculated S_{21} can be below 0.15% and $\pm 15^{\circ}$, respectively, by best selection of the values of C_t and R_t [the plot of best-fitted phase difference of S_{21} was given in Fig. 4(b)]. The degree of the error include the measurement accuracy. Nonlinearity of the WG PIN PD under high power illumination was investigated experimentally. It was found that a good linearity was kept at input power levels below 10 mW. As the optical input power was increased over 15 mW, this measurement indicated that nonlinearity is caused due to a space-charge effect. The nonlinearity of the WG PIN PD can be exactly expressed by carefully selecting the input circuit elements (C_t, R_t, and g_m) for various optical power levels. The transit time and related intrinsic 3-dB bandwidth f_t are represented with the physic parameter of the WG PIN PD as [5]

$$f_t \cong \frac{3.5 v_s}{2\pi D} \cong \frac{1}{2\pi R_t C_t} \tag{3}$$

where v_s is the carrier drift velocity due to the contributions of both hole and electron and D is the width of drift region. For the measured device, the best-fitted values $C_t = 35$ fF and $R_t = 50\ \Omega$ lead to a transit-time bandwidth f_t higher than 100 GHz. It suggests that the measured bandwidth of the WG PIN PD is mainly limited by the external parasitic RC time constant.

IV. Conclusion

In this letter, a novel equivalent circuit was proposed for the side-illuminated input tapered waveguide-integrated PIN PD. The equivalent circuit represents the carrier transit-time effect by adding a RC input circuit and voltage-controlled current source to the external RF equivalent circuit. As a result, the proposed equivalent circuit fitted well with both the measured reflection and optoelectronic conversion properties of the WG PIN PD. Most importantly, this approach allows to directly and easily evaluate the transit-time effect on high frequency photodiodes from the normally measured S parameters. The model reported in this letter can also be used as a tool for the design of PIN photodiodes for high bit rate application.

References

[1] K. Kato, "Ultrawide-band/high-frequency photodetectors," *IEEE Trans. Microwave Theory Tech.*, vol. 47, pp. 1265–1280, 1999.

[2] N. Yasuoka, M. Makiuchi, M. Miyata, O. Aoki, M. Egawa, N. Okazaki, M. Takechi, H. Kuwatsuka, and H. Soda, "High-efficiency PIN photodiodes with a spot-size converter for 40 Gb/s transmission systems," in *Proc. ECOC2001*, Sept. 30–Oct. 4, 2001, pp. 558–559.

[3] R. Sabella and S. Merli, "Analysis of InGaAs P–I–N photodiode frequency response," *IEEE J. Quantum Electron.*, vol. 29, pp. 906–916, 1993.

[4] S. Wang, *Fundamentals of Semiconductor Theory and Device Physics*. Englewood Cliffs, NJ: Prentice-Hall, 1986, p. 654.

[5] K. Kato, S. Hata, K. Kawano, and A. Kozen, "Design of ultrawide-band, high-sensitivity p–I–n-photodetectors," *IEICE Trans. Electron.*, vol. E76-C, pp. 214–221, 1993.